Journal of Electrical Engineering, Vol. 75, No. 6, 2024, pp. 522-526

sciendo
PAPERS

Partial discharge noise comparison and recognition method based on multi-channel smooth decoherence algorithm applied to GIS

Fei Du[1], Yuan Xu[1], Shuai Yuan[1], Jiangang Bi[1], Jinpeng Jiang[1], Xueqiong Zhu[2]

In order to further improve the accuracy of the online monitoring spectra of partial discharge in gas insulated switchgear, a partial discharge distributed monitoring system is studied, and distributed sensors are used to simultaneously obtain ultra-high frequency electromagnetic wave signals. Based on the accumulated partial discharge spectra of each sensor, the smooth decoherence noise recognition algorithm is proposed on a long-term cumulative spectral pattern, which is used to analyse the correlation between the spectra of each sensor. Furthermore, a method for determining whether partial discharge is an internal signal is proposed, and its effectiveness is verified by practice, the results confirmed that the algorithm can avoid the misjudgement of partial discharge results caused by distributed sensor interference.

Keywords: partial discharge, decoherence algorithm, noise recognition, spectrum recognition, state monitoring

1 Introduction

Partial discharge is a caused by deterioration of insulation medium in power equipment. The electric field distribution of power equipment is usually uneven, and high field strength areas is generated inside or on the surface of the insulation medium. Once the field strength in these areas is high enough to cause local breakdown, partial discharge will occur, and by continuously eroding the surrounding insulation medium, it will ultimately lead to discharge faults, which cause serious power grid operation accidents.

When partial discharge occurs in gas insulated switchgear (GIS), ultra-high frequency electromagnetic signals are excited [1]. By analysing the distribution pattern of electromagnetic signals in each cycle (50 Hz), partial discharge spectra can be formed to identify the type of discharge. However, in on-site applications, due to external interference from other equipment such as overhead lines, conduit clamps, welding machines, mobile phone communications, etc., such interference is usually coupled to ultra-high frequency sensors, resulting in the generation of various interference spectra by the sensors, which makes it difficult to judge whether the discharge sources are located inside the power equipment [2-4].

In the industry, wavelet denoising has become a hot research topic in the separation of partial discharge's signal-to-noise [5-8]. The combined multi-resolution ana-lysis and hard thresholding based on the non-stationary statistical characteristics' signals are widely used to form a wavelet-based transform stationary non-stationary filter (WTS-NST), experimental results show that this method can effectively separate partial discharge signals and noise signals, and has the advantages of short calculation time and small waveform distortion of extracted partial discharge signals, which is suitable for online detection of partial discharge. The time-frequency regulation characteristics of Bd wavelets combined with the time-frequency characteristics is also widely used, and the characteristics of partial discharge pulses in the wavelet domain are studied, and a method for extracting discharge pulses from strong electro-magnetic interference environments using wavelet transform was proposed, by means of which pulses are extracted from the actual measured on-site interference, demonstrating the feasibility and practicality of this method. Further, the improved wavelet transform method for continuous wavelet transform (CWT) and discrete wavelet transform (DWT) for denoising partial discharge signals are studied, which have shown that using empirical mode decomposition technology to denoise partial discharge signals in cables improves the accuracy of positioning. Although various partial discharge interference suppression techniques based on wavelet denoising have achieved good results, algorithms mainly aim to suppress periodic interference and white noise in partial discharge detection in conventional pulse current methods or high-frequency current methods [9, 10]. In practical applications, due to the large computational workload, high computational complexity, and high storage space requirements, it is not conducive to hardware implementation. In addition, wavelet denoising methods cannot suppress pulse type interference that is close to the time-frequency characteristics of discharge signals.

[1] China Electric Power Research Institute, No.15 Qinghe Xiaoying East Road, Haidian District, Beijing, China
[2] Electric Power Research Institute, State Grid Jiangsu Electric Power Co., Ltd., Nanjing 211103, Jiangsu Province, China
dufei@epri.sgcc.com.cn

https://doi.org/10.2478/jee-2024-0060, Print (till 2015) ISSN 1335-3632, On-line ISSN 1339-309X
© This is an open access article licensed under the Creative Commons Attribution-NonCommercial-NoDerivatives License (http://creativecommons.org/licenses/by-nc-nd/4.0/).

In this paper, the fast identification system for partial discharge signal and noise based on multi-channel smooth decoherence system has been designed. According to the smooth decoherence algorithm, the partial discharge signals of adjacent sensors with the same phase for equipment partial discharge alarms are calculated and compared, and the fast identification of noise signals is achieved.

2 Partial discharge distributed monitoring system applied to GIS

The partial discharge distributed monitoring system (PDDMS) consists of sensors, transmission lines, and smooth decoherence analysis modules. Taking the monitoring of gas insulated metal enclosed switchgear as an example, as shown in Fig. 1.

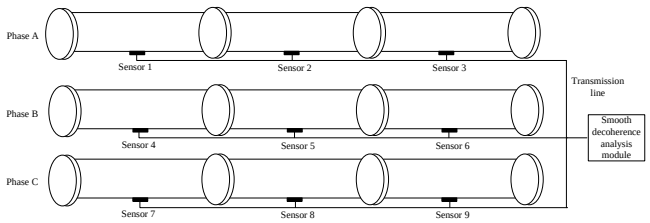

Fig. 1. Partial discharge distributed monitoring system

Partial discharge sensors 1 to 9 simultaneously collect and monitor the partial discharge signals generated inside the device. The nine signals are simultaneously transmitted to the smooth coherence analysis module via a transmission line.

The smooth decoherence analysis module takes any partial discharge sensor as a reference signal, performs smooth decoherence calculation on the remaining eight signals, and determines the correlation between each signal and the reference signal, and outputs the judgment result.

The smooth decoherence analysis module operates in the long-term cumulative spectrum recognition mode and can perform noise recognition on the long-term cumulative spectra generated by nine sensors.

3 Smooth decoherence noise recognition algorithm based on long-term cumulative spectral pattern

3.1 Spectral smoothing and coherence calculation

The total collection time T, sampling rate S, and reference sensor number K are set in PDDMS for partial discharge sampling, and PDDMS accumulates the voltage value of the i^{th} partial discharge sensor's signal at the n^{th} sampling point in the graph is shown in equation

$$\begin{cases} \varphi_0(j) = \dfrac{mod\left[\dfrac{(n-1)}{S \times 0.02}\right]}{2\pi} \\ W_i(\varphi_0(j)) = \sum_{n=1}^{T \times S} V_i(n) \end{cases} \tag{1}$$

where, $\varphi_0(j)$ is the j^{th} power frequency reference phase sequence corresponding to the n^{th} sampling point, mod is the remainder operator, and $W_i(\varphi_0(j))$ is the cumulative map of the i^{th} sensor at phase $\varphi_0(j)$. $\varphi_0(j)$ can be expressed as:

$$\varphi_0(j) = [\varphi_1, \varphi_2, \cdots \varphi_L] \quad 1 \le j \le L \tag{2}$$

Step 1: Coherence calculation without displacement

The cumulative spectrum of the i^{th} sensor signal $W_i(\varphi_0(j))$ is selected and calculated once for coherence between the i^{th} and K^{th} sensor (reference signal).

$$r_0(i,0) = \frac{L\sum_{j=1}^{L} W_i(\varphi_0(j))W_K(\varphi_0(j)) - \sum_{j=1}^{L} W_i(\varphi_0(j))\sum_{j=1}^{L} W_K(\varphi_0(j))}{\sqrt{L\sum_{j=1}^{L} W_i^2(\varphi_0(j)) - (\sum_{j=1}^{L} W_i(\varphi_0(j)))^2}\sqrt{L\sum_{j=1}^{L} W_K^2(\varphi_0(j)) - (\sum_{j=1}^{L} W_K(\varphi_0(j)))^2}} \tag{3}$$

Here, $r_0(i,0)$ represents the coherence between the cumulative spectrum of the i^{th} sensor and the cumulative spectrum of the reference signal without displacement.

Step 2: Smooth displacement

In addition to the reference signal, the data positions of the power frequency reference phase sequence and cumulative spectrum sequence generated by each sensor are shifted to the right once. The first bit of the original sequence data is moved and stored in the second bit, and so on. The last data (L^{th} data) is stored in the first bit, which can be executed according to Eqns. (4) and (5).

$$\begin{cases}\varphi_m(p) = \varphi_{m-1}(p-1) & 2 \le p \le L-1 \\ \varphi_m(1) = \varphi_{m-1}(L)\end{cases} \quad (4)$$

$$\begin{cases}W_i(\varphi_m(p)) = W_i(\varphi_{m-1}(p-1)) & 2 \le p \le L-1 \\ & i \ne K \\ W_i(\varphi_m(1)) = W_i\big(\varphi_{m-1}(L)\big) & i \ne K\end{cases} \quad (5)$$

Here, p represents the data storage location in the power frequency reference phase sequence or cumulative spectrum sequence.

Step3: Calculate the correlation after displacement

Calculate the coherence between the cumulative spectra of each sensor and the reference signal after the current smooth displacement, repeat step 2 after calculation, shift a total of (L-1) times, and terminate the shift after (L-1) times.

$$r_0(i,m) = \frac{L\sum_{j=1}^{L} W_i\big(\varphi_m(j)\big)W_K\big(\varphi_0(j)\big) - \sum_{j=1}^{L} W_i\big(\varphi_m(j)\big)\sum_{j=1}^{L} W_K\big(\varphi_0(j)\big)}{\sqrt{L\sum_{j=1}^{L} W_i^2(\varphi_m(j)) - \big(\sum_{j=1}^{L} W_i\big(\varphi_m(j)\big)\big)^2}\sqrt{L\sum_{j=1}^{L} W_K^2(\varphi_0(j)) - \big(\sum_{j=1}^{L} W_K\big(\varphi_0(j)\big)\big)^2}} \quad (6)$$

Here, m represents the number of displacements, $r_0(i,m)$ represents the coherence of spectra between the i^{th} sensor and the reference sensor after m times of displacement.

Step4: Calculate the maximum coherence of the cumulative spectrum for each sensor

The maximum coherence of the cumulative spectrum for each sensor can be obtained according to equation (7).

$$R\,max(r_0(i,m)) \quad 0 \le m \le (L-1)_{i,max} \quad (7)$$

Step5: Determination of coherence

If $R_{i,max} \ge 0.85$, it is considered that the i^{th} sensor has the same type of partial discharge as the reference sensor, which is marked as $R_{i,0} = 1$. If $R_{i,max} < 0.85$, it is considered that the i^{th} sensor is not related to the partial discharge measured by the reference sensor, which is marked as $R_{i,0} = 0$. The correlation descriptions are shown in Table 1.

Table 1. The correlation descriptions between each sensor

Coherence value	Relevance explanation	Relevance mark
$0.85 \le R_{i,max} \le 1$	The spectra of i^{th} and k^{th} sensor can be traced as the same partial discharge source or the same noise.	$R_{i,0} = 1$
$0 \le R_{i,max} < 0.85$	The spectra of i^{th} and k^{th} sensor are caused by different partial discharge source of noise.	$R_{i,0} = 0$

3.2 Comparison and judgment of partial discharge and noise signals

According to the correlation descriptions, there are three possible situations for the relevance mark, namely different situations are used to distinguish whether the discharge source is located inside or outside the device.

Situation 1: If the sensors' relevance mark $R_{i,0} = 1$ and the reference sensor is located on the same phase, but the other sensors relevance mark $R_{i,0} = 0$ in different phases, the signal received by the reference sensor is caused by a partial discharge inside the GIS, and there is a high risk of defect inside.

Situation 2: If the sensors' relevance mark$R_{i,0} = 0$ and the reference sensor is located on the same phase, and the other sensors relevance mark $R_{i,0} = 0$ in different phases, the signal received by the reference sensor might be caused by a partial discharge inside the GIS.

Situation 3: If the other sensors relevance mark $R_{i,0} = 1$ in different phases, the signal received by the reference sensor is caused by noise, namely the UHF signals outside the GIS are coupled.

Table 2. Signals' correlation with inside partial discharge

Phase	Signals' correlation		
A	$R_{1,0} = 0$	$R_{2,0} = 0$	$R_{3,0} = 0$
B	$R_{4,0} = 0$ or 1	Reference signal	$R_{6,0} = 0$ or 1
C	$R_{7,0} = 0$	$R_{8,0} = 0$	$R_{9,0} = 0$
Note: When there is a high possibility of internal defects, at least one of $R_{4,0}$and $R_{6,0}$ is 1.			

Table 3. Signals' correlation with outside noise

Phase	Signals' correlation		
A	$R_{1,0}=0$	$R_{2,0}=1$or 0	$R_{3,0}=0$
B	$R_{4,0}=0$	Reference signal	$R_{6,0}=0$
C	$R_{7,0}=0$	$R_{8,0}=1$or 0	$R_{9,0}=0$
Note: When there is noise, at least one of $R_{2,0}$ and $R_{8,0}$ is 1.			

3.3 Noise comparison and recognition in real GIS

PDDMS is used according to Fig. 1 to obtain partial discharge spectra in real GIS, the 5th sensor is selected as reference sensor, and only the second sensor receives UHF signal, the other 7 sensors receive no signal or the value is too low to trigger the acquisition card. The spectra obtained by the reference sensor and the second sensor are shown in Fig. 2.

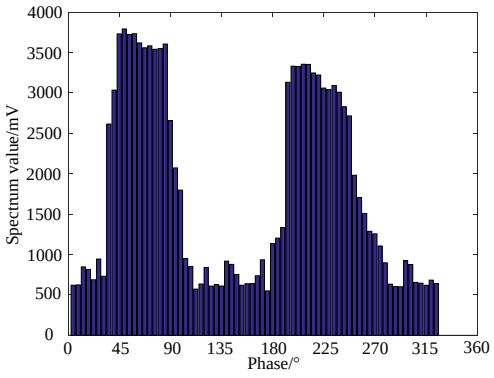

(a) Spectrum of reference sensor 5

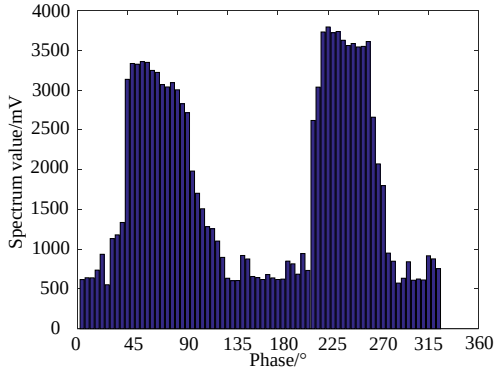

(b) Spectrum of sensor 2

Fig. 2. Spectra of partial discharge obtained by PDDMS

Since other sensors have not received effective signals, the value of $R_{i,max}$ between the reference sensor and these sensors is 0, and the value of $R_{2,max}$, namely $R_{i,0}=0$ except $R_{2,0}=1$. The correlation descriptions based on partial discharge test are shown in Tab. 4.

Table 4. Correlation descriptions based on partial discharge test

Phase	Signals' correlation		
A	$R_{1,0}=0$	$R_{2,0}=1$	$R_{3,0}=0$
B	$R_{4,0}=0$	Reference signal	$R_{6,0}=0$
C	$R_{7,0}=0$	$R_{8,0}=0$	$R_{9,0}=0$

Based on the spectra of each sensor, both spectra are concerned as insulation defect spectra, and there may be two insulation defects inside the device. After comparison and recognition, according to Table 2, the 5th and the second sensor receive the same signal, considering only noise outside of the GIS makes the sensors in different phases receive the same signal, which meets Situation 3, both of the two partial discharge spectra should be concerned as noise, namely there is no discharge signals excited by defects in GIS.

4 Conclusions

A PDDMS design method for GIS partial discharge monitoring is proposed. Based on the system, smooth decoherence noise recognition algorithm based on long-term cumulative spectral pattern, partial discharge signals of each sensor are shifted smoothly, and correlations are calculated. The algorithm proposed a quickly synchronized correlation comparison method between various sensor spectra, and quickly determine whether the signal is caused by interference or internal defects, without the need for manual intervention or on-site retesting. It provides a new solution for noise removal and diagnosis of partial discharge online monitoring in GIS.

Acknowledgement

This work is supported by Science and Technology Project of State Grid Corporation of China, Research on wide-band current array sensing technology for characterizing the operation state of main substation equipment (5200-202155419A-0-0-00).

References

[1] G. Behrmann and J. Smajic, "RF PD signal propagation in GIS: Comparing S-parameter measurements with an RF transmission model for a short section of GIS," in IEEE Transactions on Dielectrics and Electrical Insulation, vol. 23, no. 3, pp. 1331-1337, June 2016.

[2] J. A. Ardila-Rey, J. M. Martinez-Tarifa and G. Robles, "Automatic selection of frequency bands for the power ratios separation technique in partial discharge measurements: part II, PD source recognition and applications," in IEEE Transactions on Dielectrics and Electrical Insulation, vol. 22, no. 4, pp. 2293-2301, August.

[3] A. R. Mor, L. C. Castro Heredia and F. A. Muñoz, "New clustering techniques based on current peak value, charge and energy calculations for separation of partial discharge sources," in IEEE Transactions on Dielectrics and Electrical Insulation, vol. 24, no. 1, pp. 340-348, Feb. 2017.

[4] G. C. Montanari, P. Seri, R. Ghosh and L. Cirioni, "Noise rejection and partial discharge source identification in insulation system under DC voltage supply," in IEEE Transactions on Dielectrics and Electrical Insulation, vol. 26, no. 6, pp. 1894-1902, Dec. 2019.

[5] Ding and I. W. Selesnick, "Artifact-Free Wavelet Denoising: Non-convex Sparse Regularization, Convex Optimization," in IEEE Signal Processing Letters, vol. 22, no. 9, pp. 1364-1368, Sept. 2015.

[6] Y. Wu, G. Gao and C. Cui, "Improved Wavelet Denoising by Non-Convex Sparse Regularization Under Double Wavelet Domains," in IEEE Access, vol. 7, pp. 30659-30671, 2019.

[8] J. Yang, Y. Wang, W. Xu and Q. Dai, "Image and Video Denoising Using Adaptive Dual-Tree Discrete Wavelet Packets," in IEEE Transactions on Circuits and Systems for Video Technology, vol. 19, no. 5, pp. 642-655, May 2009.

[9] E. J. Balster, Y. F. Zheng and R. L. Ewing, "Combined spatial and temporal domain wavelet shrinkage algorithm for video denoising," in IEEE Transactions on Circuits and Systems for Video Technology, vol. 16, no. 2, pp. 220-230, Feb. 2006.

[10] E. A. K. Cohen and A. T. Walden, "A Statistical Study of Temporally Smoothed Wavelet Coherence," in IEEE Transactions on Signal Processing, vol. 58, no. 6, pp. 2964-2973, June 2010.

[11] J.-S. Brittain, D. M. Halliday, B. A. Conway and J. B. Nielsen, "Single-Trial Multiwavelet Coherence in Application to Neurophysiological Time Series," in IEEE Transactions on Biomedical Engineering, vol. 54, no. 5, pp. 854-862, May 2007.

Fei Du was born in Beijing, China, in 1992. He received the MS in electric and engineering from Xi'an Jiao Tong University (Xi'an) in 2017, respectively. Currently, he is an Engineer with China Electric Power Research Institute, Beijing, China. His research interests are condition monitoring of power apparatus.

Received 26 September 2024